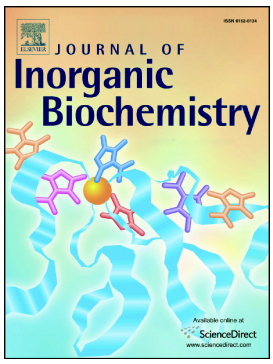

Probing the mechanism of the dedicated NO sensor [4Fe-4S] NsrR: the effect of cluster ligand environment

Erin L. Dodd, Nick E. Le Brun

PII: S0162-0134(23)00339-2

DOI: https://doi.org/10.1016/j.jinorgbio.2023.112457

Reference: JIB 112457

To appear in: *Journal of Inorganic Biochemistry*

Received date: 1 November 2023

Revised date: 11 December 2023

Accepted date: 16 December 2023

Please cite this article as: E.L. Dodd and N.E. Le Brun, Probing the mechanism of the dedicated NO sensor [4Fe-4S] NsrR: the effect of cluster ligand environment, *Journal of Inorganic Biochemistry* (2023), https://doi.org/10.1016/j.jinorgbio.2023.112457

Probing the mechanism of the dedicated NO sensor [4Fe-4S] NsrR: the effect of cluster ligand environment

Erin L. Dodd*†, Nick E. Le Brun

Centre for Molecular and Structural Biochemistry, School of Chemistry, University of East Anglia, Norwich Research Park, Norwich NR4 7TJ, UK

E-mail: dodd.erin@uqam.ca

KEYWORDS: NO sensor protein, [4Fe-4S] cluster nitrosylation, mass spectrometry coordination chemistry, biomimetic model complex

ABSTRACT

NsrR from *Streptomyces coelicolor* is a bacterial nitric oxide (NO) sensor/nitrosative stress regulator as its primary function, and has been shown to have differential response at low, mid, and high levels of NO. These must correspond to discrete structural changes at the protein-bound [4Fe-4S] cluster in response to stepwise nitrosylation of the cluster. We have investigated the effect of the monohapto carboxylate ligand in the site differentiated [4Fe-4S] cluster cofactor of the protein NsrR on modulating its reactivity to NO with a focus on indentifying mechanistic intermediates. We have prepared a synthetic model [4Fe-4S] cluster complex with tripodal ligand and one single site differentiated site occupied by either thiolate or carboxylate ligand. We report here the mechanistic details of sequential steps of nitrosylation as observed by ESI-MS and IR spectroscopy. Parallel non-denaturing mass spectrometry analyses were performed using site-differentiated variants of NsrR with the native aspartic acid, cysteine, or alanine in the position of the forth ligand to the cluster. A mono-nitrosylated synthetic [4Fe-4S] cluster was observed for the first time in a biologically-relevant thiolate-based coordination environment. Combined synthetic and protein data give unprecedented clarity in the modulation of nitrosylation of a [4Fe-4S] cluster.

1 Introduction

Nitric oxide (NO) is a freely diffusible, highly reactive gaseous small molecule with multiple roles in biology. At high concentrations NO is a cytotoxin, but at low concentrations it can act as an immune response modulator in higher eukaryotes[1-3] and an important biological inter- and intra-cellular signaling molecule in both eukaryotes and bacteria.[4-9] Elucidating the mechanisms by which organisms sense and respond to both low and toxic levels of NO, including aspects such as NO transport and repair of NO-mediated damage, can help us to understand the interplay between these systems and potentially lead to new techniques in immunotherapy.[10-12] Additionally, targeting the bacterial NO-response system could be an effective strategy to combat pathogenic infection in the current climate of rising antibiotic resistance.

In biology, metal cofactors are in general highly reactive towards NO. Proteins containing iron-sulfur (FeS) clusters are highly susceptible to NO-induced damage and nature has exploited this sensitivity in bacterial systems by employing FeS cluster proteins that function as biological switches. A family of specialized NO sensing proteins including the transcription regulatory protein NsrR have evolved in bacteria to respond to this small molecule using a [4Fe-4S] cluster that is tuned to NO reactivity. NsrR has been identified as a regulator of the NO stress response in a number of bacteria including *E. coli*[13] and the pathogen *N. gonorrhoeae*,[14] directly sensing NO in order to initiate the onset of the NO stress response, turning on the cellular NO detoxification response in the presence of NO through concomitant partial or complete nitrosylation of the FeS cluster.[4, 15] *S. coelicolor* (Sc)NsrR regulates only the *nsrR* gene itself and two *hmp* genes (*hmpA1* and *hmpA2*)[16] encoding NO detoxifying flavohaemoglobins, with differential DNA binding affinity at each of the three binding sites.

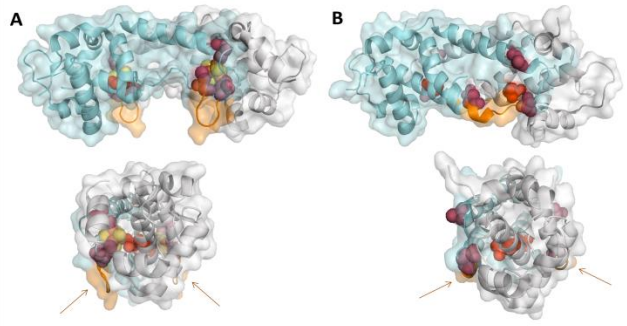

Figure 1. A and B. front and side view of holo-NsrR(A) and apo-NsrR variant C93A, C99A, C105A (B) with cluster-binding residues shown in red (Asp8) and purple (Cys/Ala93, 99, 105) and the hinged C93-C99 loop highlighted in orange. Images made using PDB IDs 5N07 and 5N08.[17]

Crack *et al*. established that the genetic turn-on response of NsrR to NO is also differentiated at 2, 4, and 8 NO molecules per cluster required to abolish binding to each of the three different gene promoter regions.[18] (Figures 1, S1) This highly specific response makes *S. coelicolor* NsrR (*Sc*NsrR) a specialized sensor of nitrosative stress. The specific NO-dependance of binding strongly suggests that specific observable nitrosylation intermediates of NsrR may be long lived, and contribute to biologically relevant structural changes in the protein as part of its NO response. Determination of which of the intermediate species that are observable experimentally are biologically relevant is a challenge. In this work we hope to gain structural insight, at

th of intermediates of nitrosylation in NsrR. In particular, we will attempt to address the question of what effect the unique coordination environment of the [4Fe-4S] cluster, with three cysteine ligands and one aspartate ligand, has on the specificity of the NsrR NO response.

Conventional thought surrounding the mechanisms of nitrosylation of iron sulfur clusters in proteins has been based largely on the known structures of synthetic model iron nitrosyl complexes, which have provided simplified systems to model the NO reactivity of the protein systems.[19-31] For ease of comparison with the synthetic cluster and discussion of synthetic clusters within this paper, we will use the formula type $[Fe_nS_m]^{0/a+/b-}$ to describe specific cluster species throughout this paper, while keeping to the traditional form [4Fe-4S] in general cases. The nitrosylation products of protein-bound iron-sulfur clusters have been identified by comparison with the spectroscopic signatures of small-molecule iron nitrosyl complexes. Nitrosylation of mononuclear iron thiolates and [2Fe-2S] cluster species results in dinitrosyl iron complex (DNIC) products (Scheme 1), while Roussin's Black Salt anion (RBS, Scheme 1), $[Fe_4S_3(NO)_7]^-$, is the major product of anaerobic nitrosylation of synthetic [4Fe-4S] clusters.

Scheme 1:

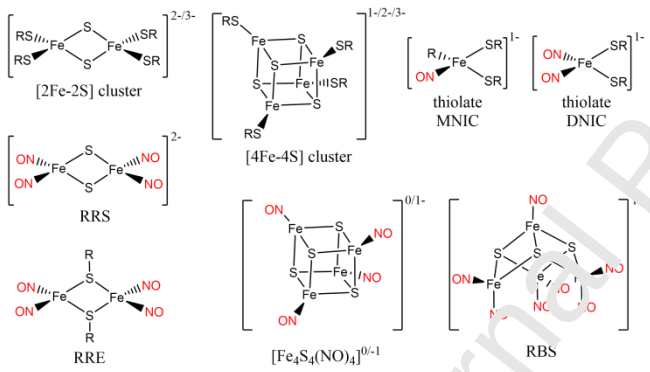

Thus far, these model studies have revealed some of the structures of mechanistic intermediates en route to these end products. The mononitrosyl iron complex (MNIC, Scheme 1) precursor to DNIC from the nitrosylation of mononuclear iron salts has been isolated.[21] The formation of DNIC from the nitrosylation of [2Fe-2S] clusters is understood to proceed through reductive elimination of the bridging sulfides as elemental sulfur, and the interconversion between DNIC and the neutral Roussin's Red Ester complex (RRE, scheme 1), $Fe_2(SR)_2(NO)_4$, has also been established.[21] [4Fe-4S] cluster nitrosylation has proven to be more complicated. A tetranitrosyl $[Fe_4S_4]^{0/1-}$ cluster complex (Scheme 1) has been established as a precursor to RBS.[20] More recently, the Suess group has reported the isolation of the mono-nitroslyated [4Fe-4S] complex $[(IMes)_3Fe_4S_4(NO)]^{0/+/2+}$ in three redox states, stablized by the neutra bulky N-heterocyclic carbene ligand IMes.[32] Other intermediates in the multistep nitrosylation of [4Fe-4S] clusters to form RBS have proven elusive to date. Mechanisms by which [4Fe-4S] cluster nitrosylation might lead to other products, such as RRE, have yet to be fully modeled synthetically. A graphic detailing the formation and mechanisms of interconversion of well-known iron nitrosyl complexes is included as Figure S2 in the supplementary data.

nitrosylation of a [4Fe-4S] ferredoxin.[33] Recent studies of the nitrosylation of the [4Fe-4S] cluster-containing Endonuclease III, another DNA-binding protein which would encounter NO while repairing DNA damaged by NO, show loss of iron and formation of stoichiometrically equal amounts of DNIC and RRE as the final nitrosylation products.[34] The Le Brun lab and collaborators have made extensive use of non-denaturing mass spectrometry (MS) and nuclear resonance vibrational spectroscopy (NRVS) to identify further products of the nitrosylation reactions of [4Fe-4S] proteins.[15, 16, 35-40] Recent NRVS studies of NsrR and another [4Fe-4S] cluster protein, WhiD, revealed a mixture of iron nitrosyl products, with RRE-like and RBS-like species as principle products, along with minor amounts of DNIC species.[36] The Le Brun lab has also recently reported in-depth analyses of nitrosylation intermediates and products of wildtype *Sc*NsrR as observed by ESI mass spectrometry and LCMS of the monomeric subunit of the protein.[37, 40] This research highlights key differences in the nitrosylation pathway of NsrR from those observed in other iron-sulfur clusters studied [15, 16, 39] However, the order of formation of these species, and the means by which the protein controls the sequential reactions of nitrosylation, remains ambiguous. In addition, the focus on the denatured monomeric subunit of the protein leads to an incomplete overall picture of the reactivity with NO, in that the monomeric subunits of dimeric NsrR are covalently bound through the coordinate colvalent Fe-$O_{(Asp)}$ bond in the cluster ligation sphere in addition to the non-covalent interactions that drive the dimerization of the apo protein. Thus disruption of the dimerization interaction between the subgroups of dimeric *holo*-NsrR would strongly affect the cluster Fe-$O_{(Asp)}$ coordination observed.

Which nitrosylation products are ultimately observed appears to be dependent reaction conditions, i.e. presence of thiols[37] or oxygen,[41] and may also be affected by [4Fe-4S] cluster environment. The recently reported crystal structure of holo-*Sc*NsrR revealed a novel ligand binding environment in which the cluster is bound by three thiolate ligands (cysteine residues Cys93, 99 and 105) located in a loop that interacts with the DNA recognition helix, and which is significantly rearranged in the absence of cluster. The fourth ligand is a carboxylate residue, Asp8, from the opposite dimer subunit.[17] The unique site-differentiated cluster ligation sphere is likely to strongly influence the relative reactivity of each iron site to NO, raising the question of to what degree the composition of the ligand environment determines the reactivity of the cluster towards NO. This hinges directly on whether the initial reaction step is one of simple ligand substitution, a redox-based step, or of a more complex rearrangement, and thus is integral to a deeper understanding of the mechanism of the reaction of NO with the NO sensor protein NsrR, and with [4Fe-4S] clusters in general.

We propose that the Asp8 ligand on the site-differentiated cluster would lead to a different, site-specific initial activity towards NO while stabilizing partially nitrosylated cluster products. It has been well established that terminal ligands of [4Fe-4S] clusters are labile to substitution, and that carboxylate ligands are more labile than thiolate ligands in a synthetic model.[42] Altering the terminal ligands has been shown to have a strong effect on the reduction potential of synthetic [4Fe-4S] clusters,[43] with carboxylate leading to a higher reduction potential than that observed for thiolate ligands alone, without perturbing the overall electronic

st[illegible] carboxylate ligand could control the type and order of structural changes in NsrR that lead to the differential NO-dependent DNA binding affinity that allows this single protein to simultaneously modulate multiple layers of nitrosylation stress response in the bacterium. To test this, the synthetic $[Fe_4S_4]^{2+}$ cluster complex developed by Terada *et al*[46] with a thiolate- or carboxylate-based ligand at the site-differentiated apical iron site were utilized here as a simplified model for the site-differentiated $[Fe_4S_4]^{2+}$ cluster in *Sc*NsrR. The tripodal trithiol ligand 'TempS_3' binds the cluster strongly, allowing us to focus on the reactivity of the differentiated site in isolation of other reactions and observe ligand-related differences in reactivity.

Understanding how nature fine-tunes the control of cluster nitrosylation may be of considerable interest in the development of agents to exploit these signaling pathways in order to control bacterial populations, with implications for the healthcare industry as well as in atmosphere and soil. We show here that key reaction intermediates of the nitrosylation of these cluster complexes are clearly observable by mass spectrometry and infrared spectroscopy. These studies were carried out alongside parallel non-denaturing mass spectrometry studies of the nitrosylation reaction of *Sc*NsrR and D8 variants of *Sc*NsrR in which the carboxylate ligand is replaced by a cysteine ligand or a non-binding alanine.

2 Materials and Methods

2.1 Wild type *Sc*NsrR and variants

Protein Purification: *Sc*NsrR and *Sc*NsrR D8A and D8C variants were expressed with C-terminal polyhistidine tags and purified anaerobically as previously described.[16, 17]

Non-denaturing Electrospray Mass Spectrometry (ESI-MS): Positive ion ESI MS under non-denaturing conditions was used to observe the nitrosylation of polyhistidine-tagged [4Fe-4S] wtNsrR and variants D8C and D8A. Electrospray ionization mass spectrometry was carried out using a Bruker micrOTOF-QIII mass spectrometer (Bruker Daltonics, Coventry, UK). The ESI-TOF was calibrated using ESI-L Low Concentration Tuning Mix (Agilent Technologies, San Diego, CA) in the positive ion mode. Acquisition of full mass spectra was controlled using Bruker oTOF Control software, with parameters as follows: dry gas flow 4 L/min, nebuliser gas pressure 0.4 Bar, dry gas 180 °C, capillary voltage 2800 V, offset 450 V, quadrupole ion voltage 15 V, collision RF 650-750 Vpp, collision cell voltage 5 V. Processing and analysis of MS experimental data were carried out using Compass DataAnalysis version 4.1 (Bruker Daltonik, Bremen, Germany). Neutral mass spectra were generated using the ESI Compass version 1.3 Maximum Entropy deconvolution algorithm over a mass range of 34500 – 36500 Da. Mass accuracy was ± 1 Da.

Sample preparation for ESI-MS: Solutions of protein were prepared anaerobically by buffer exchange from the storage buffer into 50 mM NH_4OAc, pH 7.4 via 10 mL PD10 desalting column (GE Healthcare) followed by dilution. The concentration of cluster-containing protein was determined approximately using the reported extinction coefficient ε_{406} = 13.3 ± 1 $mM^{-1}cm^{-1}$.[16] Variation in cluster absorbance among variants was presumed to be small. Dipropylenetriamine (DPTA) NONOate (10 mg) from Cayman Chemicals was dissolved in aqueous NaOH (1.0 mL, 1 M). At the start of the

d the concentration of NO released was determined roughly using the NONOate half-life of 3.0 hours at 37 °C at pH 7.4. The solutions were mixed quickly and transferred to a Hamilton gastight syringe needle held at 37 °C for the duration of the reaction. This experimental design was chosen over the addition of individual aliquots of NO delivery agent because minimizing manipulations and transfers between anaerobically sealed vessels allowed for minimization of risk of introducion of oxygen.

Nitrosylation reaction followed by ESI-MS: Following purging of the instrument with anaerobic buffer (ammonium acetate 50 mM, pH 7.4), samples were introduced as anaerobic buffer solution (*ca*. 500 μM) at a flow rate of 5 $\mu L min^{-1}$ using a syringe pump. Reaction solutions were infused directly (0.3 ml/hr) into the ESI source of a Bruker micrOTOF-QIII mass spectrometer (Bruker, Coventry, UK) operating in the positive ion mode. Full mass spectra (*m/z* 50 – 3500) were recorded for 5 min. Spectra were combined, processed using the ESI Compass 1.3 Maximum Entropy deconvolution routine in Bruker Compass Data analysis 4.1 (Bruker Daltonik GmbH). The mass spectrometer was calibrated with ESI-L low concentration tuning mix (Agilent Technologies).

2.2 Synthetic clusters

All reagents were purchased from Sigma Aldrich UK or Thermo Fisher Scientific UK unless otherwise specified. ^{1}H- and ^{13}C-NMR spectroscopy was performed on a Bruker Ascend 500 (500 MHz) instrument. FT-IR spectra were measured using a Bruker FT-IR XSA spectrometer. Elemental analysis was carried out at London Metropolitan University using a Thermo Scientific Flash 2000 Elemental Analyzer configured for % CHN. All solvents for anaerobic synthesis and analysis excepting NMR were freshly distilled anaerobically according to standard methods.

1,3,5-Tris(bromomethyl)-2,4,6-triethylbenzene **(1)**: Triethylbenzene (50 mmol) was combined with paraformaldehyde (550 mmol), zinc bromide (85 mmol), and HBr/AcOH (30 wt %, 100 mL), diluted with a further 100 mL AcOH, and heated to 90 ^{0}C overnight with vigorous stirring. Upon cooling, 100mL of water was added and the mixture stirred for a further hour. Finally the mixture was poured into 500 mL water and the grey-white crystals of (1) were collected by filtration and dried under vacuum to give off-white crystalline solid (1) in 95 % yield. 1H NMR (CDCl3) δ 4.59 (s, 6H), 2.96 (q, J = 7.5 Hz, 6H), 1.36 (t, J = 7.5 Hz, 9H). Spectroscopic match to literature values.[47, 48]

1,3,5-Tris(2-methoxybenzyl)-2,4,6-triethylbenzene **(2)**: 2-bromoanisole (40 mmol) was added to a suspension of magnesium powder (100 mmol) in THF (50 mL) under N_2. 1-3 crystals of iodine were added, and the mixture stirred at room temperature for 2 h. This Grignard solution was then added by filter cannula transfer into a reaction mixture containing 1 (10 mmol) and CuI (5 mmol) in THF (25 mL) stirring under nitrogen. The combined solutions were heated to 60 ^{0}C overnight, cooled to room temperature, quenched with aqueous $NaHCO_3$, and the crude product was extracted with DCM, dried over $MgSO_4$, filtered through a silica plug, and isolated *in vacuo* as a white crystalline solid in 60 % yield. 1H NMR (CDCl3) δ 7.16 ppm (t, J = 7.63 Hz, 3H), 6.87 ppm (d, J = 7.63 Hz, 3H), 6.80 ppm (t, J = 7.96 Hz, 3H), 6.59 ppm (d, J = 7.96 Hz, 3H), 4.03 ppm (s, 6H), 3.92 (s, 9H), 2.34 ppm (q, J = 7.54 Hz, 6H), 1.13 ppm (t, J = 7.54 Hz, 9H).

1,3,5-Tris(5-(acetylthio)-2-methoxybenzyl)-2,4,6-triethylbenzene (Temp(SAc)$_3$) (**3**): N-bromosuccinimide (80 mmol) was added to a solution of (2) (10 mmol) in methyl ethyl ketone (100 mL) and stirred under N_2 for 24 hours at 60 ^{0}C. Upon cooling to room temperature, aqueous H_2SO_4 (100 mL, 1M) was added, the reaction was stirred for a further 30 min open to atmosphere, then the organic phase was separated with DCM, washed with saturated aqueous NaCl, dried over $MgSO_4$, filtered through a silica plug, and isolated in vacuo as a white powder in 70 % yield. ^{1}H NMR ($CDCl_3$) δ 7.26 ppm (dd, J1 = 8.61 Hz, J2 = 2.48 Hz, 3H), 6.73 ppm (d, J = 8.61 Hz, 3H), 6.67 ppm (d, J = 2.48 Hz, 3H), 3.99 ppm (s, 6H), 3.90 ppm (s, 9H), 2.30 ppm (q, J = 7.61 Hz, 6H), 1.12 ppm (t, J = 7.61 Hz, 9H). Spectroscopic match to literature values.[46]

1,3,5-Tris(5-mercapto-2-methoxybenzyl)-2,4,6-triethylbenzene (Temp(SH)$_3$) (**4**): A solution of compound **3** (1.846 g, 2.4 mmol) in thf (60 mL) was cooled to -78 ^{0}C under N_2. *n*BuLi (16 mL, 1.6 M in hexanes) was added slowly dropwise. The reaction mixture was stirred for 3 hours at -78 ^{0}C then stirred at 0 ^{0}C for a further 5 hours. S_8 (0.486 g, 1.9 mmol) was added at -78 ^{0}C under a flow of N_2 and the reaction mixture was stirred overnight at room temperature. The following day, $LiAlH_4$ (1 g) was added slowly under a flow of N_2, and stirred for 8 hours. Water was added (40 mL), followed by HCl (100 mL, 1 M) and extracted with DCM. The organic fraction was dried over $MgSO_4$, filtered through a silica plug, and isolated in vacuo as a white powder (1.075 g, 1.7 mmol, 70 % yield. ^{1}H NMR ($CDCl_3$) δ 7.14 ppm (dd, J1 = 8.33 Hz, J2 = 2.29 Hz, 3H), 6.76 ppm (d, J = 8.33 Hz, 3H), 6.54 ppm (d, J = 2.29 Hz, 3H), 3.97 ppm (s, 6H), 3.90 ppm (s, 9H), 3.60 ppm (s, 3H), 2.27 ppm (q, J = 7.6 Hz, 6H), 1.18 ppm (t, J = 7.6 Hz, 9H). Spectroscopic match to literature values.[46]

[(Fe$_4$S$_4$(SEt)$_4$](PPh$_4$)$_2$ (**5**)*:* Sodium ethanethiolate (48 mmol) was dissolved in methanol (40 mL) under N_2 and stirred for 10min at room temperature. Iron (III) chloride (10 mmol) was dissolved in methanol (40 mL) and added under N_2 to the first solution, to form a purple-brown solution which was stirred for 1 hour at room temperature. Sulfur (10.1 mmol) was added under a flow of N_2 and the resulting dark brown solution was stirred overnight. The following day tetraphenylphosphonium chloride (10 mmol) was dissolved in methanol (10 mL) under N_2. The dark brown solution containing the Fe complex was transferred into this flask by positive pressure cannula filtration and the resulting solution sealed under N_2 and stored in a freezer at -20 ^{0}C without stirring overnight. The following day, the supernatant was removed by positive pressure cannula filtration, and the residual black crystalline solid was washed with cold methanol (5x 20 mL). The black crystals were then dried in vacuo. Elemental anal. (%) calculated: C 52.76; H, 4.74; Found C 52.54, H 4.86. Spectroscopic match to literature.[49]

[(Fe$_4$S$_4$(TempS$_3$)(SEt)](PPh$_4$)$_2$ **(6)**: (Prepared as per literature)[46] Compound **4** (1.075 g, 1.7 mmol) was dissolved in thf (35 mL) and added to a solution of **5** (2.06 g, 1.7 mmol) in acetonitrile (25 mL) under N_2. The solutions were combined by cannula transfer and stirred overnight at room temperature under N_2. The solvent was then removed *in vacuo*, and the resulting black solid was washed with thf (5x 10 mL) and dried *in vacuo* (2.15g, 1.2 mmol, 70% yield). Elemental anal. (%) calculated: C 60.45; H 5.02; Found C 55.57; H 5.08. Spectroscopic match to literature.

[(Fe$_4$S$_4$(TempS$_3$)(COOEt)](PPh$_4$)$_2$ (**7**): (Prepared as per literature)[50] Propionic acid (5 mL, 67 mmol) was added to a stirred for 4 hr followed by removal of solvent and volatiles *in vacuo*. The residue was washed with a 1:1 ether:THF mixture and extracted by acetonitrile (15 mL). Removal of the solvent *in vacuo* gave **7** as a black powder

Preparation of anhydrous NO reagent solution: NO gas was purified by passing through packed ascarite and bubbling through 5M aqueous NaOH. The solubility of NO in MeCN is $14.1x10^{-3}$ $Matm^{-1}$, compared to the solubility in water at pH 7.0, which is $1.8x10^{-3}$ $Matm^{-1}$.[51, 52]

IR and ESI-MS: individual samples were pre-prepared prior to analysis: samples of 1.5 mM [Fe$_4$S$_4$(TempS$_3$)(SEt)](PPh$_4$)$_2$ or [Fe$_4$S$_4$(TempS$_3$)(OCOEt)](PPh$_4$)$_2$ in acetonitrile were prepared anaerobically inside an MBraun glovebox under N_2 atmosphere and sealed in 2 mL septa-capped vials to which were subsequently added the appropriate volume of saturated NO solution in anaerobic acetonitrile. Saturated NO solution was prepared by bubbling freshly distilled anaerobic acetonitrile with a gas mixture of purified 10% NO in N_2 (BOC industrial gases UK) for 20 min, and transferred via Hamilton gastight syringe.

ESI-MS was carried out using a Bruker micrOTOF-QIII mass spectrometer (Bruker Daltonics, Coventry, UK) with the following parameters: dry gas flow 4 L/min, nebuliser gas pressure 0.4 Bar, dry gas 180 °C, capillary voltage 2400 V, offset 500 V, quadrupole ion voltage 5 V, collision RF 400 Vpp, collision voltage 10 V. Following purging of the instrument with anaerobic acetonitrile, pre-mixed samples were introduced as anaerobic acetonitrile solution (*ca*. 500 μM) at a flow rate of 5 μL/min using a syringe pump. Negative ion ESI MS was used. To obtain an approximation of sequential addition of nitric oxide to [4Fe-4S]-cluster sample, a saturated solution of NO in dry, anaerobic acetonitrile was prepared by bubbling a 10% gas mixture of NO in N_2 for 30min. This solution was added in aliquots to solutions of cluster compound in acetonitrile (1.000 mL, 1.5mM) and introduced to the instrument via Hamilton gastight syringe.

Liquid-phase infrared spectroscopy was carried out using a Bruker FT-IR XSA spectrometer. A sealed Omni fixed liquid IR cell fitted with two 2 mm CaF_2 windows separated by a 50 μm PTFE spacer was flushed with anaerobic acetonitrile, followed by injection of pre-mixed samples in anaerobic acetonitrile solution.

3 Results

3.1 The influence of cluster coordination sphere on nitrosylation of the [4Fe-4S] NsrR dimer

The effect of altering the carboxylate ligand to the cluster of *Sc*NsrR on the nitrosylation reaction has been previously explored spectroscopically, and at that time we reported[17] significant differences in the rate of initial reactivity of the wild type protein as compared to the D8C and D8A variants in which the native cluster-bound carboxylate-bearing aspartic acid residue was altered to a cysteine and a non-binding alanine respectively. The reaction rates were found to be affected by the substitution, with D8A > wild type > D8C. CD absorbance spectroscopy showed a different pattern of proteinfolding for the D8C variant over the course of the nitrosylation reaction as compared to the other variant and the native protein. Furthermore, differences in the NO reactivity of NsrR and the [4Fe-4S] cluster protein WhiD, which

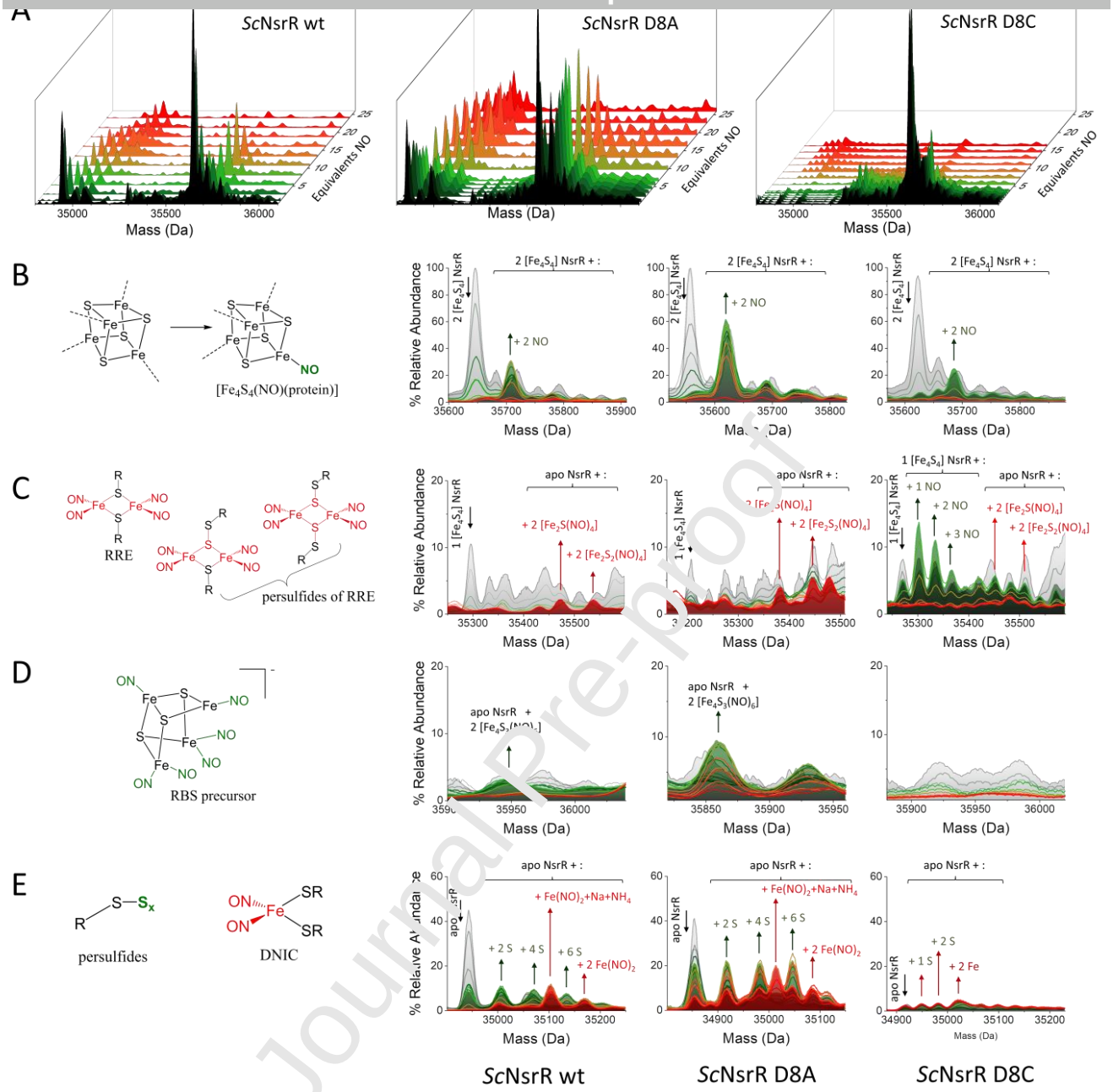

Figure 2: The influence of cluster coordination on nitrosylation of the [4Fe-4S] NsrR dimer: A. Non-denaturing mass spectrometry titration of three variants of NsrR (wild type, D8A, and D8C) against NO shows the effect of the 4th cluster ligand on determining the type and longevity of nitrosylated intermediates in the protein dimer region of the mass spectrum. NO was sourced from the timed-release compound DPTA NONOate sufficient to release 26 equivalents of NO over approximately 3 hours. Wt *Sc*NsrR shows formation of a few distinct product peaks in the holo-dimer range and apo-dimer range; the D8A variant shows intermediate products are more long-lived, while the D8C variant shows complete reaction at much lower levels of NO overall. B-E: Close-up analysis of overlaid MS spectra of the three variants of [4Fe-4S] NsrR (0-2 equiv. NO shown in gray, 2-10 equiv. NO shown in green, 10-26 equiv. NO shown in red for clarity) and major product assignments based on previous work from the Le Brun laboratory [40]: B. The holo-dimer region for protein with both cluster sites occupied shows evolution and subsequent diminuation of mononitrosylated species at both [4Fe-4S] cluster sites on the NsrR dimer is conserved for wt and D8A but is especially short-lived in D8C; C. Possible persulfide species are observed at both sites on NsrR dimer for all species, while sequential nitrosylation of single [4Fe-4S] cluster observed in dimeric D8C NsrR with only one cluster site occupied reveals significant early-stage nitrosylation products with 1, 2, and 3 NO bound in only the D8C variant; D. There is minimal contribution of dimeric protein with both clusters converted to RBS, but there is clear evidence of a product consistent with a 6-NO derivative of RBS; E. the apo-dimer region shows extensive formation of persulfide and polysulfide species, with DNIC products observed late in nitrosylation in the wt and D8A variants but not the D8C variant.

coordinates its cluster by four cysteines, have been observed by NRVS and MS.[36, 37, 40] The presence of a carboxylate ligand in the coordination environment of the NsrR cluster is potentially a major factor in the differential reactivity. The

and its effect on the nitrosylation mechanism as observable through ESI mass spectrometry.

Non-denaturing mass spectrometry (MS) couples soft electrospray ionisation (ESI) and Time of Flight (TOF) detection with solution and ionization conditions under which proteins remain folded and other non-covalent interactions and sensitive cofactors are preserved. This enables accurate mass detection of intact proteins and protein complexes. ESI mass spectrometry is emerging as a powerful tool for the study of sensitive iron sulfur cluster holoproteins.[53-56] The NO-releasing molecule DPTA-NONOate (Dipropylenetriamine NONOate or 3,3′-(Hydroxynitrosohydrazino)bis-1-propan-amine) has a well-defined half-life of 180 minutes at 30 °C and pH = 7.4 to release two molecules of NO for each molecule of NONOate. Following the MS of each NsrR variant combined with 30 equivalents of NONOate under NO-liberating conditions over a three hour period allowed for detailed observation of the nitrosylation products formed over the course of the reaction. Previous studies were focused on a monomeric form of NsrR resulting from dissociation of the native dimer, which aided assignment of nitrosylated species.[37, 40] Previously reported data in the mass range of dimeric NsrR were not of sufficiently high resolution to be useful. Here we have optimized conditions in order to obtain suitably high resolution mass data for the dimeric form of wild type NsrR and variants.

Mono- and dinitrosylated species:

Comparing the three variants in the early stages of the reaction, we find that the mono-nitrosylated species $[[Fe_4S_4(NO)](NsrR)]_2$ is far more long-lived in the D8A and wild type protein, persisting even up to 15 equivalents of NO per cluster compared to 5 equivalents of NO in the case of the D8C (Figure 2A, Table S1). This species is assigned as +2 NO in Figure 2A, representing one NO ligand per cluster of the dimeric protein. For all variants, $[[Fe_4S_4(NO)](NsrR)]_2$ is observed as the mass of apo protein +760 Da (or holo protein + 60 Da), and interpreted as one NO ligand (+1 NO, 30 Da) per cluster.

We were unable to ascertain with certainty whether a dinitrosylated species, $[[Fe_4S_4(NO)_2](NsrR)]_2$ (+4 NO, or apo + 820 Da) was present at low NO levels, due to overlap with a peak at apo + 830 Da (where holo refers to the observed mass of the apo protein plus the added mass of two [4Fe-4S] clusters) attributed to two additional S^0 atoms per monomeric unit. This peak was present in the initial protein spectrum. In the wild type protein the tri-nitrosylated species, $[[Fe_4S_4(NO)_3](NsrR)]_2$, or +6 NO, may be present at apo + 882 Da as a band with weak intensity, but this is unclear as it is obscured by overlap with another peak. Likewise, the tetra-nitrosylated species $[[Fe_4S_4(NO)_4](NsrR)]_2$, predicted by synthetic studies to be a major intermediate in the nitrosylation pathway, may be present at quite low peak intensities at apo + 942 Da but this too is unclear. Neither the tri nor the tetra-nitrosylated species were identified in previous studies.

In the D8A variant, the evolution of the mono- and di-nitrosylated species bound to dimeric protein is observable in approximately the same pattern as that seen in the wild type (Figure 2A, Table S1). These intermediates appear more long-lived under the reaction conditions and/or MS conditions than their counterparts in wild type NsrR against further nitrosylation reaction, with more intense mass peaks relative reaction period.

In the D8C variant, the mono-nitrosylated cluster is evident at up to 5 equivalents of NO, but the reaction pathway seems to differ from that observed in the other variants at higher levels of NO. Intermediates in the mass range up to + 250 Da above the holo dimer peak are difficult to distinguish for this variant, as there are many additional products observed. These may correspond to unevenly-nitrosylated cluster pairs, with $[[Fe_4S_4(NO)_2][Fe_4S_4(NO)](NsrR)_2]$ (+ 3 NO, apo + 790 Da) and $[[Fe_4S_4(NO)_3][Fe_4S_4(NO)_2](NsrR)_2]$ (+ 5 NO , apo + 850 Da) possibly accounting for the peaks in these positions (Figure 2A, Table S1). Additionally, in the D8C variant $[[Fe_4S_4(NO)](NsrR)_2]$ (+ 1 NO, apo + 380 Da), $[[Fe_4S_4(NO)_2](NsrR)_2]$ (+ 2 NO, apo + 410 Da), $[[Fe_4S_4(NO)_3](NsrR)_2]$ (+ 3 NO, apo + 440 Da), and $[[Fe_4S_4(NO)_4](NsrR)_2]$ (+ 4 NO, apo + 500 Da) are clearly observed in a protein dimer with only a single cluster site occupied (Figure 2B, Table S1).

The asymmetrical formation of nitrosylation products across the dimer pair appears to be evidence of each cluster in the dimer being nitrosylated at rates independent of the other subunit, which we did not see in the site-differentiated variants. Firstly, the observation of asymmetrical behaviour in one of the variants confirms that our deconvolution methods have not artificially produced a false set of 'dimer' peaks as artifacts (supplementary information). If that was the case, we would observe symmetric behaviour across the dimer pair for all three variants. Secondly, it tells us that there is something in particular about the dimeric structure and/or coordination environment of the wild type and D8A variants that causes the clusters to be nitrosylated in a coordinated way, such that, for example, when one cluster reacts to become bound to a single nitrosyl, the other cluster in the dimer must immediately become bound to one as well, in order that we would never see the singly-nitrosylated dimer. This could arise from cooperativity in iron nitrosyl formation for these variants.

All three variants have$[Fe_2S(NO)_4]_2$, apo protein + 528 Da, as a major component of the final product mixture (Figure 2B, Table S1). This is a match for the group identified and confirmed by isotope substitution in earlier studies of the wild type protein as a persulfide-linked RRE-like $[Fe_2S(NO)_4]$ species at apo + 264 Da in the monomeric NsrR[37, 40], with one RRE-like cluster in each cluster site. The previous isotope study discounts the alternative assignment of a single, unsymmetrical RBS, $[Fe_4S_3(NO)_7]$ (apo protein + 530 Da). A persulfide-linked RRE-type complex would be indicative of a cluster rearrangement, from bridging sulfides to bridging thiolates/perthiolates. This mechanism is supported by the observation of an apo + 592 Da peak assigned as two $[Fe_2S_2(NO)_4]$ units symmetrically positioned across a dimer pair. The sulfur atoms may be expected to be bridging, and bound to the cysteine ligands as persulfides (Figure 2C). This species would be a reasonable precursor to $[Fe_2S(NO)_4]$ through loss of a sulfide.

RBS-like species have been observed in prior studies of NsrR nitrosylation.[40] The dimer with symmetrically-bound RBS units would be expected at apo + 1056 Da (Figure 2C, Table S1), as a minor product of nitrosylation of wild type NsrR.[37] This peak, if present, is too small to assign with certainty for the wild type or D8C variants of NsrR. A peak at apo + 1076 Da observed in the D8A variant is assigned to a dimer with two RBS units and an NH_4^+ adduct. A peak at + 996 Da is

nitrosylation of the synthetic model complex discussed later in this manuscript. $[Fe_4S_3(NO)_6]^-$ was identified by Bourassa et al. as a product of flash photolysis of RBS that readily re-combined with NO to give back RBS.[57]This suggests that the $[Fe_4S_3(NO)_6]^-$ may be either a stable intermediate *en route* to the RBS which may not remain bound to protein, or else a stable RBS-like species in its own right, which is able retain its bond to protein through the free coordination site on the cluster. The $[Fe_4S_3(NO)_6]^-$ is notable as an RBS precursor because it would have one coordinatively unsaturated tetrahedral iron. In the synthetic complex we predicted that an NO ligand could be present as a bridging ligand to stabilize the structure. A $[Fe_4S_3(NO)_6]$ unit bound to the protein via a pendant cysteine thiolate could thus be a precursor poised to release from the protein upon nitrosylation and either be ejected from the protein as RBS or to begin the cluster sulfide loss and rearrangement process towards thiolate-bridged DNIC species, dependent on the concentration of mediating thiols in the cellular environment.

The D8A variant cluster incorporation is slightly lower than that of wild type, and a higher proportion of apo protein in the sample is associated with a larger apo peak in the mass spectrum. This is not sufficient to account for the prevalence of cluster-free persulfide species in the D8A following nitrosylation. We see + 2 S (+ 64 Da), + 4 S, and + 6 S, observed as sequential increments of + 64 from the apo dimer peak, forming immediately and remaining major species until more than 12 equivalents of NO per FeS cluster have been added (Figure 2D, Table 1 S). The dimeric units gain persulfides equally; there are no significant + 1 S, + 3 S, or + 5 S peaks at fewer than 10 equivalents of NO per cluster. Adducts of the apo protein are only seen in small quantities in the D8C, indicating higher affinity for maintaining bonds to its cluster. In fact the D8C has a significantly different profile in this region, with sulfide addition occurring unevenly across dimer pairs such that we see dimer pairs with + 1 S, + 2 S, and possibly + 5 S and higher, observed as sequential increments of + 32 Da from the apo dimer peak (Figure 2D, Table 1S).

At above 18 equivalents NO per cluster, far beyond the stoichiometric requirement for complete nitrosylation of all iron sites in the protein, the wild type and D8A variants both give a pair of products at apo + 160 Da and apo + 232 Da whose structures are likely related because they grow in together at the same point in the titration. These are tentatively assigned as DNIC adducts, as previously reported.[40] The peak at apo + 232 Da is assigned to a single $[Fe(NO)_2]$ adduct in each of the two FeS cluster binding sites. The peak at + 160 Da may arise from the corresponding asymmetrically-substituted protein dimer with only one site occupied by $[Fe(NO)_2]$, with sodium and ammonium ions for charge balance accounting for the added mass. While the most likely site for these DNIC species is the original cluster ligation site, there may also be a slight possibility of capture of liberated iron nitrosyl species by the C-terminal polyhistidine tags of the protein, which would give the same mass. Alternatively + 160 Da could be interpreted as two Fe and two Na atoms, which would be a more symmetric distribution across dimer subunits, or five S atoms. The DNIC assignment is preferred due to the confirmation of DNIC products as observed in the monomeric protein.[37, 40] Isotope distribution studies of nitrosylation of the monomeric NsrR subunit support the single-site DNIC species.[40] This is a significant finding, as wild type and D8A dimers begin to react asymmetrically, but symmetrical reactivity, which could be interpreted as cooperative, is maintained at lower NO levels.

3.2 The influence of cluster coordination sphere on nitrosylation of synthetic [4Fe-4S] clusters

In order to attempt to observe the controlled nitrosylation of a [4Fe-4S] cluster at a single iron site, we utilized the site-differentiated [4Fe-4S] cluster system developed by Terada *et al*.[46, 50] in which the tripodal ligand has been observed to stabilize the cluster with carboxylate ligands in the apical ligand site. We observed the nitrosylation of thiolate and carboxylate analogs of this cluster using ESI mass spectrometry and infrared spectroscopy.

The tripodal trithiol ligand, previously reported as $Temp(SH)_3$,[46] was synthesized according to an alternative method (Scheme S1), reducing the overall number of steps and reliance on air- and moisture-sensitive chemistry. The tri-brominated tripodal base of the ligand was prepared using literature methods.[47, 48] Cu(I) – catalyzed coupling between the Grignard reagent formed from 2-bromoanisole and 1,3,5-tris(bromomethyl)-2,4,6-triethylbenzene connecting the base to the coordinating arms of the ligand, adapted from a similar synthesis in the literature,[58] provided a simple and elegant regiospecific route to the tripodal scaffold, with high yield and no discernible partially-substituted product. N-bromosuccinimide brominated the 5 position of the 'arms' with high yield and selectivity,[59, 60] and the final substitution to give the trithiol ligand was adapted from the original $Temp(SH)_3$ ligand synthesis. Lengthening of reported reaction times led to a substantial yield increase compared to the initial report, and the final product was found to have low sensitivity to oxidation once isolated in crystalline form.

The $[Fe_4S_4(SEt)_4]^{2+}$ cluster was obtained by self-assembly using standard methods,[49] and recrystallized as the tetraphenylphosphonium salt (5). Room temperature incubation of stoichiometric quantities of cluster complex and tripodal ligand $TempS_3$ afforded the monoethanethiolate $TempS_3$ ligated complex (6) upon recrystallization. Subsequently, application of the ligand exchange procedure of Terada *et al*.[50] using propionic acid afforded the carboxylate complex (7) (Scheme S2).

Observation of synthetic $[Fe_4S_4(SR)_4]^{2-}$ complexes by electrospray mass spectrometry (ESI MS) is not new, nor is the use of ESI MS to monitor a ligand substitution reaction of similar clusters. Hoveyda and Holm[61] used ESI MS to observe the stepwise substitution of 1-4 SH^- ligands on the cluster species $[Fe_4S_4(SH)_4]^{2-}$ for the more nucleophilic *p*-$CF_3C_6H_4S^-$ and, importantly, found that at low cone voltages where fragmentation was minimal, the ratio of intensities of the anions was the same as the ratio of intensities observed via NMR spectroscopy, highlighting the usefulness of ESI MS for accurate representation of the ratio of species in a reaction mixture at the time of sampling. More recently, a combination of mass spectrometry and infrared spectroscopy was used to verify that a tetra-nitrosylated cluster $[Fe_4S_4(NO)_4]^-$ is an intermediate in the formation of Roussin's black salt from a synthetic [4Fe-4S] cluster.[20]

In this work, the reactivity of the $[Fe_4S_4(TempS_3)(SEt)]^{2-}$ complex to nitric oxide was studied by negative ion ESI MS titration, using saturated NO solutions in acetonitrile as the NO source (Figure 3). All the species of isolated FeS clusters

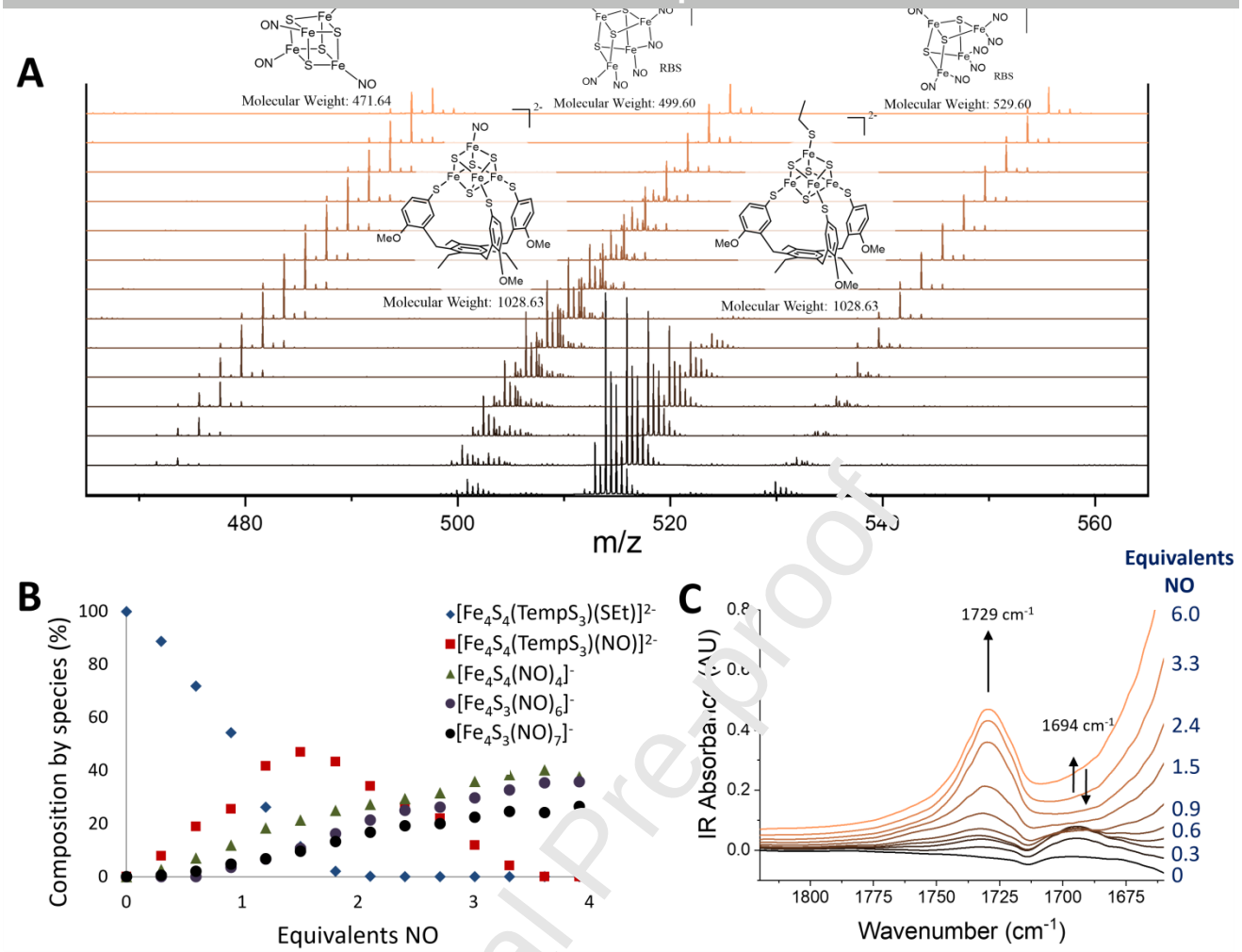

Figure 3. Nitrosylation of $[Fe_4S_4(TempS_3)(SEt)]^{2-}$ followed by mass spectrometry in the negative ion mode. A. Expansion of the *m/z* 460 – 540 region shows major species evolution clearly with easily discernible isotope patterns aiding in characterization. No fragmentation peaks were observed under these conditions. Stacked plots are offset for clarity. B. Species composition over course of titration as a function of nitric oxide stoichiometry. Equivalents of NO as per [Fe4S4] cluster. Approximate relative species composition was determined using the area of the plot over the range occupied by the isotope distribution pattern for each species as a measure of that species' contribution. C. Nitrosylation of $[Fe_4S_4(TempS_3)(SEt)]^{2-}$ followed by solution phase IR shows growth of a nitrosyl band at ν_{NO} 1729 cm^{-1}, with a second band at 1694 cm^{-1} growing in in the early stages of reaction and then disappearing.

discussed here were readily observable as intact molecular ion peaks in the negative ionization mode of the mass spectrometer and characterized by mass-charge ratio and isotope pattern (Figures S13, S17). The parent ion $[Fe_4S_4(TempS_3)(SEt)]^{2-}$ was observed at *m/z* 514, together with a small amount of the ion-paired species $[[Fe_4S_4(TempS_3)(SEt)](PPh_4)]^-$ (*m/z* 1368). Such ion-paired species are commonly observed for multiply-charged anions.[62] No discernible oxidized species of the cluster was observed.

The anion at *m/z* 501 with isotope pattern consistent with bound tripodal ligand and a single chloride was tentatively assigned as $[Fe_4S_4(TempS_3)(Cl)]^{2-}$ based on the isotope distribution pattern. This peak was present in MS of the unreacted $[Fe_4S_4(TempS_3)(SEt)]^{2-}$ and was possibly a result of a small amount of free chloride impurity within the instrument leading to some chloride ions reacting with intact molecular ions that had lost the apical ligand. Increasing the ionization voltage increased the intensity of these peaks relative to the molecular ion peak. In-source CID (collision-induced dissociation) fragmentation of the molecular ion peak resulted in the formation of higher-order clusters at higher energies. These clusters were artifacts of the more extreme experimental conditions and not relevant to the biological cluster reactions.

At low levels of NO, a species at m/z 499 emerged which was characterized as the singly-nitrosylated species $[Fe_4S_4(TempS_3)(NO)]^{2-}$ based on isotope distribution and mass (Figure S14), with the relative abundance of $[Fe_4S_4(TempS_3)(NO)]^{2-}$ being maximal at one equivalent NO and reducing at higher NO levels. A small amount of the ion-paired species $[[Fe_4S_4(TempS_3)(NO)](PPh_4)]^-$ was also observed at m/z 1337, with peak intensity proportional to that of the $[Fe_4S_4(TempS_3)(NO)]^{2-}$ peak at each spectrum over the course of the titration. We saw no sign of intermediates with more than one NO bound to the cluster with tripodal ligand. Supporting this, the monoanionic coordinatively unsaturated di- and tri- nitrosylated cluster intermediates $[Fe_4S_4(NO)_2]^-$ and $[Fe_4S_4(NO)_3]^-$ are observed, though the low abundances

lack of higher-order nitrosylated [4Fe-4S] intermediates bound to the $TempS_3$ ligand suggests strongly that the tripodal ligand is lost before a dinitrosylated species is formed. At higher degrees of nitrosylation, we observed only the tetranitrosylated species $[Fe_4S_4(NO)_4]^-$ at *m/z* 471 and Roussin's black salt adducts $[Fe_4S_3(NO)_6]^-$ at *m/z* 500, and $[Fe_4S_3(NO)_7]^-$ at *m/z* 529. A very small amount of NO-free $[Fe_2S_2(TempS_3)]^-$ species is observed at *m/z* 792. This species is initially observed at greater than 1 NO per cluster, and decreases again at greater than 2 equivalents. No induced dissociation of cluster-bound NO or aggregation to higher-order clusters was observed in these species under these conditions.[63]

Parallel studies of the same reaction as followed by solution phase IR spectroscopy revealed an initial band at 1694 cm^{-1} which increased at low levels of NO but decreased again as the concentration approached 0.3 equivalents NO. A band at 1729 cm^{-1} was more long-lived, and present at all NO concentrations tested, up to 3 equivalents, which was assigned as the known species $[Fe_4S_4(NO)_4]^-$.[20] Based on the MS data, we have tentatively assigned the 1694 cm^{-1} band as the NO stretch (ν_{NO}) of the mono-nitrosylated species $[Fe_4S_4(TempS_3)(NO)]^{2-}$. At 1694 cm^{-1}, the frequency of this band is lower than the ν_{NO} = 1728 cm^{-1} assigned to the IMes-stabilized mononitrosylated [4Fe-4S] cluster species of equivalent redox state reported by Suess.[32] This is rationalized by a rough comparison of the relative electronic effects of the ligands at the other three Fe sites: the N-heterocyclic carbene IMes of the Suess complex is a neutral σ-donor, similar to imidazole-type ligands but with stronger σ-donor character,[64] while the thiolates of the $TempS_3$ ligand (our complex) are negatively-charged ligands with both σ donor and π-donor character. Stronger electron-donating effects by the other three ligands would have a lengthening effect on the bound NO ligand, and therefore lead to a lower frequency ν_{NO} for the complex. Of those iron nitrosyl species for which infrared characterization is well established, no significant contributions from RBS species were observed at low concentrations of NO, nor were any DNIC or RRE species observed. A large band at 1630 cm^{-1} that increased with NO additions was also present in the spectrum of the stock solution of NO, and was ascribed to free NO in acetonitrile. Clearly the reaction of NO with cluster is either sufficiently slow or in equilibrium such that a sub-stoichiometric NO levels, much of the NO remains unreacted.

Crack *et al* found that nitrosylation of *Sc*NsrR in the presence of the biologically relevant thiols glutathione and mycothiol by LC-MS resulted in the observation of Roussin's Red Ester (RRE) – like species in which nitrosylated cluster remained bound to protein.[37] We were interested to see if this effect could be replicated in the synthetic species. We found that performing the simple titration against NO in the presence of excess thiol, in this case ethanethiol, had a protective effect, with the parent species observed at nearly unchanged concentration at 1 equivalent NO, and remaining the dominant species up to 5 equivalents NO. The amount of $[Fe_4S_4(TempS_3)(NO)]^{2-}$ remained low (Figure S16), while the tetranitrosyl $[Fe_4S_4(NO)_4]^-$ was present at high concentrations well before the emergence of the higher-order nitrosyls. An additional species, $[Fe_4S_4(SEt)(NO)_3]^-$, was also observed in the presence of excess ethanethiol. The concentration of intermediates remained low throughout the experiment, with RBS contribution finally rising sharply at the point where the Notably, no sign of RRE-like or persulfide species was observed. The evolution of ethane dithiol could not be detected by MS as the molecular weight was too low.

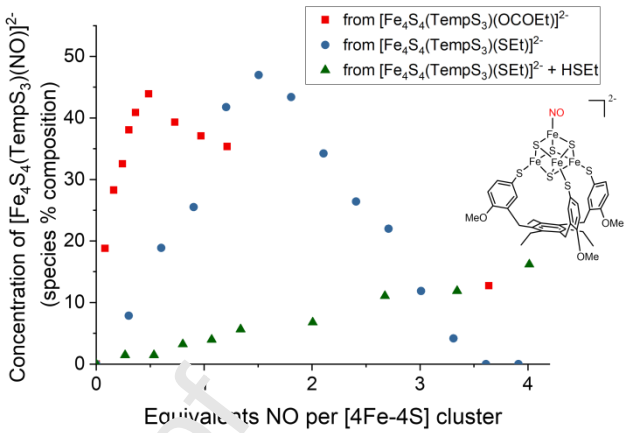

Figure 4: Comparison of formation of mononitrosylation product $[Fe_4S_4(TempS_3)(NO)]^{2-}$ from the synthetic model starting materials $[Fe_4S_4(TempS_3)(OCOEt)]^{2-}$ (red squares), $[Fe_4S_4(TempS_3)(SEt)]^{2-}$ (blue circles) and $[Fe_4S_4(TempS_3)(SEt)]^{2-}$ in the presence of excess thiol HSEt (green triangles) in mass spectrometry experiments by stoichiometry shows dependence on affinity and availability of competing ligands. Some points were omitted from this representation because they were too overlapped to quantify.

In the absence of a thiolate ligand that can act as sulfide scavenger as well as electron donor, the reaction required more NO per cluster to obtain the same intermediates. The nitrosylation of the propionate-bound synthetic cluster $[Fe_4S_4(TempS_3)(OCOEt)]^{2-}$ (Figure S18) gave the same species of intermediates as that of the ethanethiolate cluster, and reached a maximum concentration of mononitrosylated intermediate $[Fe_4S_4(TempS_3)(NO)]^{2-}$ at approximately one NO per cluster, but the tetranitrosylated species $[Fe_4S_4(NO)_4]^-$ dominated from one to nearly twenty equivalents of NO (Figure S18). This result was treated tentatively, as the propionate cluster showed evidence of a large amount of the chloride impurity in the MS data (Figure S17). The chloride-bound cluster seemed to be consumed by reactivity with NO alongside the propionate, though at a lower rate (Figures S17, S18).

With a reduction potential of 90 mV higher than that of the ethanethiolate cluster complex,[50] we expect the carboxylate complex to be a better electron acceptor, and thus for addition of nitrosyl to be a more favoured reaction while the carboxylate is still bound. Once displaced, however, the propionate ion cannot affect the reaction further. The mass spectrometry results clearly indicate that, at least in the case of these specific clusters in which the other three sites are strongly bound to the tridentate aryl thiolate ligand, the site-differentiated ligand is the first to be displaced in all cases.

The stability of the mononitrosyl species against further nitrosylation is in fact lower for the propionate cluster than the thiolate cluster (Figure 4). The binding affinity of carboxylate for the cluster may be lower than that of thiolate. In addition, this effect might be partially explained by the stabilizing effect caused by adding excess thiol to the reaction mixture, as the displaced thiolate could play the same protective role, possibly

by competing for NO directly.

MS is only able to report on long-lived intermediates in the nitrosylation, thus we are unable to discern between a concerted mechanism of initial ligand displacement for the initial displacement of SEt by NO, in which both ligands would be bound in a transition state, or a non-concerted, S_N1-type mechanism. No peak at *m/z* 1058 or 529 consistent with an isotope distribution for a species $[Fe_4S_4(TempS_3)(NO)(SEt)]^{1-/2-}$ was observed at any point over the course of titration, and we conclude that there is no observable intermediate with SEt and NO bound at once. Likewise, no peak was observed at *m/z* 967, indicating an absence of observable $[Fe_4S_4(TempS_3)]^{1-}$, or molecular ion lacking a ligand on the site-differentiated ion.

4 Discussion

The formation of the initial mono-nitrosylated species is a key step in the nitrosylation mechanism. Stable mono-nitrosylated intermediates are observed in the synthetic $TempS_3$-ligated cluster and all three variants of NsrR. The control of the formation and stability of this initial species in the protein does seem to be related to the cluster chelation environment, through a combination of control of the site of first ligand displacement, and by the tuning of the reduction potential of the cluster and thereby altering the reactivity. Which of these factors is of more relevance in NsrR is partially addressed by the data obtained in our synthetic model studies.

The observed $[Fe_4S_4(TempS_3)]^-$ mono-nitrosyl species observed by MS is dianionic. Under the gentle ionization conditions used, the observed species charge is expected to reflect the charge of that species outside the MS, as was seen for the other known species observed in our MS experiments. Since NO is a neutral radical species and the leaving group thiol is anionic, the formation of this species requires a redox event to have taken place to supply the $[Fe_4S_4(TempS_3)(NO)]^{2-}$ with an additional electron, with either the NO converted to nitroxyl prior to reaction, or a concomitant redox event at the time of substitution, such as that described in Scheme 3. In this scheme we propose that nitrosyl substitution could potentially be coupled with ultimate oxidation of the thiolate rather than the cluster itself. The cluster is expected to be involved in mediating the redox process, effectively facilitating the transfer of an electron from the thiolate to the NO.

Free thiol or thiolate is the most likely electron donor in the simplified model system. The oxidation of thiols to disulfides when the electron acceptor is molecular oxygen can be catalyzed by a wide variety of agents including [4Fe-4S] cluster compounds.[65] NO-mediated oxidation of NsrR cysteine residues to disulfides was observed in previous studies.[37, 40] Moreover, mass spectrometric analysis has conclusively confirmed the evolution of disulfide and persulfide adducts of NsrR bound to glutathione or mycothiol following the reaction of the protein with NO in the presence of an excess of the thiol at pH 8.[37] Formation of persulfide-bound FeS clusters from cysteine-bound clusters is a known motif in the literature more generally[66] and persulfide-bound cluster has been observed crystallographically.[67] This is strong evidence for this mechanism to be a factor in the evolution of iron nitrosyl products in the protein-NO reaction. In the previous work describing the product formation of NsrR-bound iron nitrosyls in the presence of added thiol in the was of the RRE type, with masses consistent with apo + $[Fe_2(NO)_4]$ implying loss of the bridging sulfide.[37]

Here we have shown that excess thiol inhibits formation of FeS cluster nitrosyl products in synthetic clusters where ligand inflexibility precluded formation of RRE products. Fitzpatrick *et al* have established that the presence or absence of excess thiolate can drive the product formation of FeS cluster nitrosylation towards DNIC/RRE and RBS products respectively.[68-71] Our results show conclusively that this trend extends to biologically-relevant clusters and is very likely to be a part of biological significance in the thiol-rich cytoplasm of *S. coelicolor* and other bacteria.

Scheme 2

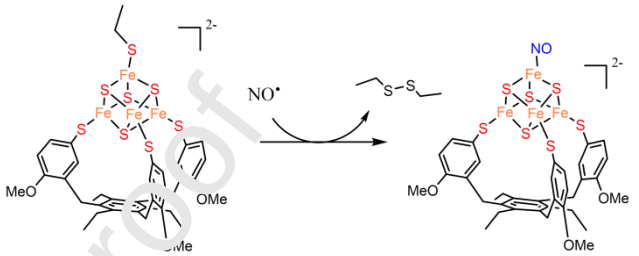

Further evidence for the biological significance of this mechanism is found in the evolution of different product types when the protein is nitrosylated in different redox environments. In a cellular environment where endogenous thiol compounds such as mycothiol are plentiful,[37] the thiol may act as both as a source of electrons in the formation of the initial mono-nitrosylated complex, and as a scavenger of oxidized S^0 when the cluster loses bridging sulfides at higher levels of nitrosylation.

The reduction potentials of $[Fe_4S_4]^{2+}$ clusters are heavily dependent on its ligand environment in a manner that correlates strongly with the degree of electron withdrawing ability of the ligand.[43] Clusters with aromatic thiolate ligands have reduction potentials that are positively shifted in comparison with clusters with aliphatic thiolate ligands for example, which brings them closer to the relatively positive reduction potentials observed in protein-bound clusters of the ferredoxin type, usually found within the range -0.1 to -0.6 V.[72] Clusters with mixed thiolate ligand spheres will have reduction potentials in between those extremes.[73] The model clusters, with a reduction potential of -0.95 V vs NHE for the thiolate (applying a conversion factor of +0.54 V to the reported value of -1.49 V vs $Ag/AgNO_3$ reference electrode)[46] and a reduction potential near -0.86 V vs NHE for the propionate cluster (same conversion)[50] are therefore likely to be poorer electron acceptors than the cysteine-ligated cluster in the protein, in addition to other differences in reaction environment. While this suggests that the predicted reduction event would be accessible to the protein cluster, some care must therefore be taken not to over-interpret the formation of dianionic mono-nitrosylated cluster as indicative that the same reaction mechanism would occur in NsrR.

The ligand environment of NsrR includes a carboxylate ligand to the site-differentiated iron, which, in synthetic clusters, is reported to give a 90 mV positive shift in reduction potential compared to an otherwise equivalent complex with ethanethiolate in the site-differentiated position.[50] This means that the site-differentiated cluster with apical carboxylate is a better electron acceptor. Bond lengths and

of the synthetic complex[46] and holo-NsrR[17] are equivalent within the range of error, implying that the protein ligand environment would be expected to exhibit the same behavior. Carboxylate, as a hard mono-hapto ligand, is electron-withdrawing in nature, while the soft thiolate ligand is electron-donating. The hydrogen bond between D8 and R12 revealed by the crystal structure would be expected to enhance the electron-withdrawing effect even further. A more positive reduction potential in the cluster of NsrR could be a key factor in the specificity of this protein's response to NO.

We can predict that, of the three variants of NsrR explored here, presuming otherwise similar protein structure as is suggested by CD spectroscopy,[17] D8C NsrR would have a more negative reduction potential as compared to wild type. The fourth ligand in the case of the D8A is not known. Compared to the wild type protein, which follows a clear nitrosylation pathway with a clear progression of nitrosylation products, D8C reacts with NO non-specifically, with products in which one cluster was lost entirely from the dimer observed alongside the formation of the expected lower nitrosyl products.

Although the D8C variant was found to have reacted completely at much lower levels of NO, the *initial* rate of reaction for the D8C was the slowest of the three variants as determined by rate analysis using stopped flow spectroscopy.[17] The titration showed complete loss of cluster at sub-stoichiometric levels of NO. This points to site access, rather than a redox event, as potentially initially rate limiting for the binding of the first nitrosyl.

The relative affinity of the cluster for nitrosyl as compared to the D8 ligand has also been shown to be crucial to the reactivity of the apical iron. The D8A variant, for which no strongly bound ligand at the 4th cluster iron is expected, followed a pathway very similar to that of the wild type protein. The actual ligand at this site is at this time unknown. No evidence was seen of iron lability, as in aconitase. This suggests that there is a ligand present to prevent the Fe lability. An adventitious water or acetate ligand from the buffer would be the most likely potential ligands, which could be potentially stabilized by the surrounding H-bonding network in that region of the protein structure.[17] The initial rate of reaction was fastest for the D8A variant[17] consistent with a more open pathway through the protein for the incoming gas molecule, a more open site, and a less tightly-bound leaving group for the initial chelation of the first nitrosyl. Similar reaction pathways for the D8A and wild type protein provide added support for the hypothesis that the D8-bound Fe is the site of initial NO binding as predicted by the cavity map of the crystal structure of the holo-protein.[17] The mechanism of nitrosylation observed for wild type and D8A NsrR is necessarily independent of the structure imposed by the hydrogen bond between D8 and R12, essential for DNA binding but absent in the D8A variant. This clarifies the observation that the D8A variant does not bind DNA.

However, this does not fully address the question of why the later stages of nitrosylation are more controlled in the wild type, while the D8C reacts to completion at lower levels of NO, and shows evidence of asymmetrical nitrosylation across the clusters. The key to answering this question may be found in analyzing how nitrosylation would disrupt the structure at the interface of the dimer pair of the protein without complete loss of dimerization.

DNA affinity in the wild type protein. NsrR, however, has differential DNA affinity at different levels of nitrosylation such that its affinity for discrete binding sites is altered while affinity for other binding sites is maintained. This differential DNA affinity must correspond to at least three discrete isolatable partially-nitrosylated complexes. The coordination environment of the FeS cluster for each species would be pivotal in shaping the dimeric protein's secondary structure and thereby leading to a differential regulatory response to different cellular levels of NO. For this reason, the differential reactivity between the D8C, D8A, and wild type protein dimers against nitrosylation supports a hypothesis that control of the reactivity is imparted by the aspartate ligand of the wild type. Previously reported circular dichroism (CD) spectroscopy experiments with this variant set used to follow changes in protein folding showed that the spectral pattern of the unreacted D8C differed from that of the other variants. When the nitrosylation of each of the variants was followed over time, the D8C again diverged and showed a very different spectral pattern at lower levels of NO, but at very high levels of NO the CD spectrum of D8C became similar to those of the other variants. The wt and D8A followed a much more similar pattern of spectral changes throughout the reaction as followed by CD spectroscopy.

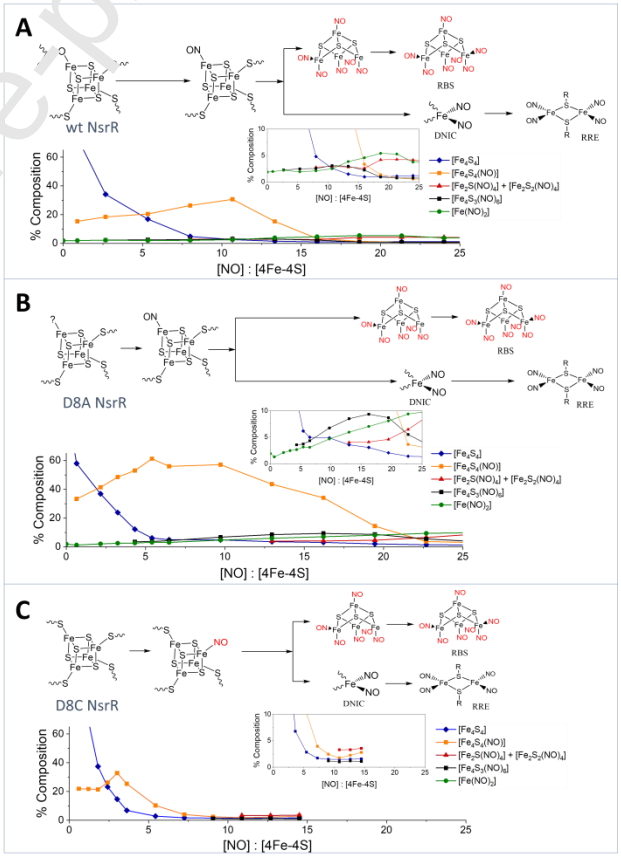

Figure 5: Comparison of formation of nitrosylation products in mass spectrometry experiments by stoichiometry (equivalents NO) from the three NsrR variant models, wild type NsrR (A); D8A NsrR (B); D8C NsrR (C), show dependence on cluster ligand type. Complexes products followed in this figure include mononitrosylated cluster $[Fe_4S_4(NO)(protein)]$ (orange); combined species $[Fe_2S(NO)_4]$ and $[Fe_2S_2(NO)_4]$ (red); $[Fe_4S_3(NO)_6]$ (black); and DNIC species $[Fe(NO)_2]$ (green).

fourth ligand to its [4Fe-4S] cluster. The carboxylate forms a monodentate bond with the cluster Fe , with the other oxygen of the carboxylate engaged in a H-bonding interaction with Arg12 on the same α-helix α1.[17] Synthetic model studies with a synthetic site-differentiated [4Fe-4S] cluster with a library of carboxylate ligands with and without crystallographically-observed intra- and inter-molecular H-bonds have established that the H-bonding interactions render the carboxylate ligand more labile to dissociation than carboxylate ligands without H-bonding interactions, and also more labile than thiolate ligands.[50]

Thus we have learned that a thiolate ligand disrupts the nitrosylation pathway significantly, while the variant with no ligand at all on the site-differentiated Fe (that we know of) produces a protein that seems to have longer-lived intermediates and seems less reactive towards NO, despite having the presumably more accessible cluster site and the highest initial rate of reaction.[16] Recall that in the absence of a protein-bound ligand, the D8A variant cannot link its dimer subunits covalently through the Asp-Fe linkage, and would also have lost the structurally important H-bonding interactions of Asp8 observed in the crystal structure of holo-NsrR.[17] Instead, D8A dimerizes solely through hydrogen bonding and other Van der Waals forces. The D8A would therefore be expected to have a much more accessible cluster. Thus we conclude that controlling the mechanism of cluster nitrosylation cannot depend strictly on controlling or restricting access to the site-differentiated site, but in fact may arise from increasing that access.

In a protein structure, this would also be possible, but the structure of the protein would hold the binding carboxylate close enough to the site of the cluster such that re-association could also be possible in the absence of other factors. If the dissociation event occurs, the secondary structure of the protein with disassociated carboxylate ligands would have to alter in its folding to accommodate the positional shift of the carboxylate. A protein where the bound carboxylate is in equilibrium with the dissociated carboxylate would experience a consequent equilibrium of these two structural states. The first nitrosylation event at the site differentiated Fe would prevent re-association of the carboxylate ligand at the cluster site, and also prevent a return to the 'bound' structure of the surrounding amino acids. Because the carboxylate ligand is located on the other dimer subunit, it is likely that a shift in the position of Asp8 away from the cluster would push α1 away from the cluster as well. This structural change could hypothetically even induce a structural change as far away as the other cluster in the dimer, a distance of approximately 30 Å. Although this hypothesis is untested crystallographically, the complete absence of asymmetrically nitrosylated clusters in dimeric wt and D8A NsrR provides strong support for some form of cooperativity in the binding.

The all-thiolate D8C variant, on the other hand, would have no ligand with differential lability, and therefore its cluster would have no differential reactivity at any Fe in the cluster, because none of the sites would have a ligand poised to dissociate. Thus it is the D8C variant, and not the D8A, which reacts with NO in a less controlled manner.

We have determined experimentally that (i.) the presence of a labile ligand is important for the protein to maintain controlled, concerted nitrosylation across both clusters, and that (ii.) the initial formation of the mononitrosylated complex

cluster in the model cluster complex, and possibly in the protein as well. These two factors are far from independent. Following a cluster reduction made more facile by the electron withdrawing effect of the H-bonded carboxylate, the binding affinity of the carboxylate to the cluster Fe would be reduced, leading to increased chance of dissociation, which would open a binding site for nitrosylation. Thus these two effects could easily be connected and vital to the tight control wtNsrR shows over the nitrosylation mechanism of its [4Fe-4S] clusters.

5 Conclusions

Though the identification of the tetranitrosyl species $[Fe_4S_4(NO)_4]^-$ as an intermediate en route to the formation of RBS has been well-established in the literature,[20] we report here the first clear observation of a synthetic mono-nitrosylated [4Fe-4S] cluster species in which the three other liganads to the [4Fe-4S] are thiolates, mimicking the cluster environment of naturally-occuring [4Fe-4S] ferredoxins. The mono-nitrosylated [4Fe-4S] cluster is clearly a biologically relevant, relatively stable complex in the nitrosylation pathway, and access to a simplified model of this nitrosylation product opens doors to a better understanding of the control of reactivity exhibited by proteins such as NsrR that has been so difficult to reproduce synthetically in the past. Further work is underway to exploit this opportunity, especially towards isolation of a crystal structure and clear IR signature of this important complex.

Overall the similarity of the nitrosylation pathway of the synthetic models to that of the protein-bound clusters is confirmed, re-enforcing the usefulness of these complexes as model systems. This is important, as we have also established here that the ligand environment is crucial to the fine-tuning of the cluster response to NO. Many bacterial species contain NsrR, and organisms from all phyla contain iron-sulfur cluster proteins. Certainly nitric oxide is a known signaling molecule in a wide range of species, and its biological activity is tightly tied into redox regulation and transfer via biological thiols as S-nitrosothiols. It is probable that this controlled response to NO by FeS proteins is represented more widely in biology, and is therefore an important mechanism to understand in a more general sense. Through careful choice of ligand environment, nature is able to direct the nitrosylation pathway to control reactivity and reactive site specificity such that specific nitrosylation steps are accompanied by specific discrete structural conformations of the protein. In this way, the otherwise unspecific, messy nitrosylation reaction becomes a useful tool in nature's toolbox.

ASSOCIATED CONTENT

Supporting information includes synthetic characterization data, further MS and IR data, and larger images of protein MS data. Supplementary data to this article can be found online at https://doi.

AUTHOR INFORMATION

Corresponding Author

* E-mail: dodd.erin@uqam.ca

Present Addresses : †**Current address for Erin L. Dodd:** Département de Chimie, Université du Québec à Montréal, C.P. 8888, Succursale Centre-Ville, Montréal (Québec), H3C 3P8, Canada

This work was supported by the Royal Society through the Newton International Postdoctoral Fellowship Fund, awarded to ELD under host NLB, as well as the Biotechnology and Biological Sciences Research Council Grants (BB/J003247/1 and BB/P006140/1). The authors would like to thank Prof. Chris Pickett of the University of East Anglia for synthetic lab space and instrumentation. We also acknowledge the influence of unpublished results by Eric Victor and Stephen J. Lippard of the Massachusetts Institute of Technology.

REFERENCES

[1] D.A. Wink, H.B. Hines, R.Y.S. Cheng, C.H. Switzer, W. Flores-Santana, M.P. Vitek, L.A. Ridnour, C.A. Colton, Journal of Leukocyte Biology, vol. 89, 2011, pp. 873-891.
[2] T.J. Guzik, R. Korbut, T. Adamek-Guzik, J. Physiol. Pharmacol., vol. 54, Polish Physiological Society, 2003, pp. 469-487.
[3] P.M. Thwe, E. Amiel, Cancer Lett, vol. 412, 2018, pp. 236-242.
[4] J.C. Crack, Green, J., Hutchings, M. I., Thomson, A. J., and Le Brun, N. E., Antioxidants & Redox Signaling, vol. 17, 2012, pp. 1215–1231.
[5] F.X. Guix, I. Uribesalgo, M. Coma, F.J. Muñoz, Progress in Neurobiology, vol. 76, 2005, pp. 126-152.
[6] T.L. Krukoff, Brain Research Reviews, vol. 30, 1999, pp. 52-65.
[7] R.M.J. Palmer, A.G. Ferrige, S. Moncada, Nature, vol. 327, Nature Publishing Group, 1987, pp. 524.
[8] B.M. Henares, K.E. Higgins, E.M. Boon, ACS Chemical Biology, vol. 7, American Chemical Society, 2012, pp. 1331-1336.
[9] K. Cosby, K.S. Partovi, J.H. Crawford, R.P. Patel, C.D. Reiter, S. Martyr, B.K. Yang, M.A. Waclawiw, G. Zalos, X. Xu, K.T. Huang, H. Shields, D.B. Kim-Shapiro, A.N. Schechter, R.O. Cannon Iii, M.T. Gladwin, Nature Medicine, vol. 9, Nature Publishing Group, 2003, pp. 1498.
[10] A. Vazquez-Torres, F.C. Fang, EcoSal Plus, American Society for Microbiology, 2014, pp. 1-18.
[11] C.A. Vaine, R.J. Soberman, Adv. Immunol., vol. 121, Elsevier Inc., 2014, pp. 191-211.
[12] Q.-G. Ding, J. Zang, S. Gao, Q. Gao, W. Duan, X. Li, W. Xu, Y. Zhang, Drug Discov Ther, vol. 10, 2017, pp. 276-284.
[13] J.D. Partridge, D.M. Bodenmiller, M.S. Humphrys, S. Spiro, Molecular Microbiology, vol. 73, 2009, pp. 680-694.
[14] K. Heurlier, M.J. Thomson, N. Aziz, J.W.B. Moir, Journal of Bacteriology, vol. 190, 2008, pp. 2488-2495.
[15] J.C. Crack, M.R. Stapleton, J. Green, A.J. Thomson, N.E. Le Brun, Journal of Biological Chemistry, vol. 288, 2013, pp. 11492-11502.
[16] J.C. Crack, J. Munnoch, E.L. Dodd, F. Knowles, M.M. Al Bassam, S. Kamali, A.A. Holland, S.P. Cramer, C.J. Hamilton, M.K. Johnson, A.J. Thomson, M.I. Hutchings, N.E. Le Brun, Journal of Biological Chemistry, vol. 290, 2015, pp. 12689-12704.
[17] A. Volbeda, E.L. Dodd, C. Darnault, J.C. Crack, O. Renoux, M.I. Hutchings, N.E. Le Brun, J.C. Fontecilla-Camps, Nature Communications, vol. 8, The Author(s), 2017, pp. 15052.
[18] J.C. Crack, D.A. Svistunenko, J. Munnoch, A.J. Thomson, M.I. Hutchings, N.E. Le Brun, Journal of Biological Chemistry, 2016.
[19] T.-T. Lu, C.-C. Tsou, H.-W. Huang, I.J. Hsu, J.-M. Chen, T.-S. Kuo, Y. Wang, W.-F. Liaw, Inorganic Chemistry, vol. 47, American Chemical Society, 2008, pp. 6040-6050.
[20] E. Victor, S.J. Lippard, Inorganic Chemistry, vol. 53, American Chemical Society, 2014, pp. 5311-5320.
[21] Chemical Society, vol. 128, American Chemical Society, 2006, pp. 3528-3529.
[22] T.C. Harrop, D. Song, S.J. Lippard, Journal of Inorganic Biochemistry, vol. 101, 2007, pp. 1730-1738.
[23] T.C. Harrop, Z.J. Tonzetich, E. Reisner, S.J. Lippard, Journal of the American Chemical Society, vol. 130, American Chemical Society, 2008, pp. 15602-15610.
[24] C.E. Tinberg, Z.J. Tonzetich, H. Wang, L.H. Do, Y. Yoda, S.P. Cramer, S.J. Lippard, Journal of the American Chemical Society, vol. 132, American Chemical Society, 2010, pp. 18168-18176.
[25] Z.J. Tonzetich, L.H. Do, S.J. Lippard, Journal of the American Chemical Society, vol. 131, American Chemical Society, 2009, pp. 7964-7965.
[26] T.-T. Lu, S.-J. Chiou, C.-Y. Chen, W.-F. Liaw, Inorganic Chemistry, vol. 45, American Chemical Society, 2006, pp. 8799-8806.
[27] I.J. Hsu, C.-H. Hsieh, S.-C. Ke, K.-A. Chiang, J.-M. Lee, J.-M. Chen, L.-Y. Jang, G.-H. Lee, Y. Wang, W.-F. Liaw, Journal of the American Chemical Society, vol. 129, American Chemical Society, 2007, pp. 1151-1159.
[28] C.-C. Tsou, T.-T. Lu, W.-F. Liaw, Journal of the American Chemical Society, vol. 129, American Chemical Society, 2007, pp. 12626-12627.
[29] C.-C. Tsou, Z.-S. Lin, T.-T. Lu, W.-F. Liaw, Journal of the American Chemical Society, vol. 130, American Chemical Society, 2008, pp. 17154-17160.
[30] T.-T. Lu, H.-W. Huang, W.-F. Liaw, Inorganic Chemistry, vol. 48, American Chemical Society, 2009, pp. 9027-9035.
[31] Z.-S. Lin, F.-C. Lo, C.-H. Li, C.-H. Chen, W.-N. Huang, I.J. Hsu, J.-F. Lee, J.-C. Horng, W.-F. Liaw, Inorganic Chemistry, vol. 50, American Chemical Society, 2011, pp. 10417-10431.
[32] Y. Kim, A. Sridharan, D.L.M. Suess, Angewandte Chemie International Edition, vol. 61, 2022, pp. e202213032.
[33] Z.J. Tonzetich, H. Wang, D. Mitra, C.E. Tinberg, L.H. Do, F.E. Jenney, M.W.W. Adams, S.P. Cramer, S.J. Lippard, Journal of the American Chemical Society, vol. 132, American Chemical Society, 2010, pp. 6914-6916.
[34] L.A. Ekanger, P.H. Oyala, A. Moradian, M.J. Sweredoski, J.K. Barton, Journal of the American Chemical Society, vol. 140, American Chemical Society, 2018, pp. 11800-11810.
[35] J.C. Crack, J. Green, A.J. Thomson, N.E.L. Brun, Accounts of Chemical Research, vol. 47, American Chemical Society, 2014, pp. 3196-3205.
[36] P.N. Serrano, H. Wang, J.C. Crack, C. Prior, M.I. Hutchings, A.J. Thomson, S. Kamali, Y. Yoda, J. Zhao, M.Y. Hu, E.E. Alp, V.S. Oganesyan, N.E. Le Brun, S.P. Cramer, Angewandte Chemie International Edition, vol. 55, 2016, pp. 14575-14579.
[37] J.C. Crack, C.J. Hamilton, N.E. Le Brun, Chemical Communications, vol. 54, The Royal Society of Chemistry, 2018, pp. 5992-5995.
[38] J.C. Crack, D.A. Svistunenko, J. Munnoch, A.J. Thomson, M.I. Hutchings, N.E. Le Brun, Journal of Biological Chemistry, vol. 291, 2016, pp. 8663-8672.
[39] J.C. Crack, L.J. Smith, M.R. Stapleton, J. Peck, N.J. Watmough, M.J. Buttner, R.S. Buxton, J. Green, V.S. Oganesyan, A.J. Thomson, N.E. Le Brun, J. Am. Chem. Soc., vol. 133, American Chemical Society, 2011, pp. 1112-1121.
[40] J.C. Crack, N.E. Le Brun, Chemistry – A European Journal, vol. 25, 2019, pp. 3675-3684.
[41] D.B. Grabarczyk, P.A. Ash, W.K. Myers, E.L. Dodd, K.A. Vincent, Dalton Transactions, vol. 48, The Royal Society of Chemistry, 2019, pp. 13960-13970.
[42] R.W. Johnson, R.H. Holm, Journal of the American Chemical Society, vol. 100, American Chemical Society, 1978, pp. 5338-5344.

[4 ic Society, vol. 145, American Chemical Society, 2023, pp. 10376-10395.
[44] Y.-J. Fu, X. Yang, X.-B. Wang, L.-S. Wang, Inorganic Chemistry, vol. 43, American Chemical Society, 2004, pp. 3647-3655.
[45] X.-B. Wang, S. Niu, X. Yang, S.K. Ibrahim, C.J. Pickett, T. Ichiye, L.-S. Wang, Journal of the American Chemical Society, vol. 125, American Chemical Society, 2003, pp. 14072-14081.
[46] T. Terada, T. Wakimoto, T. Nakamura, K. Hirabayashi, K. Tanaka, J. Li, T. Matsumoto, K. Tatsumi, Chem. - Asian J., vol. 7, Wiley-VCH Verlag GmbH & Co. KGaA, 2012, pp. 920-929.
[47] A. Vacca, C. Nativi, M. Cacciarini, R. Pergoli, S. Roelens, Journal of the American Chemical Society, vol. 126, American Chemical Society, 2004, pp. 16456-16465.
[48] M. Martin, G. Gasparini, M. Graziani, L.J. Prins, P. Scrimin, European Journal of Organic Chemistry, vol. 2010, WILEY-VCH Verlag, 2010, pp. 3858-3866.
[49] B.A. Averill, T. Herskovitz, R.H. Holm, J.A. Ibers, Journal of the American Chemical Society, vol. 95, American Chemical Society, 1973, pp. 3523-3534.
[50] T. Terada, K. Hirabayashi, D. Liu, T. Nakamura, T. Wakimoto, T. Matsumoto, K. Tatsumi, Inorganic Chemistry, vol. 52, American Chemical Society, 2013, pp. 11997-12004.
[51] C.L. Young, Solubility Data Ser., vol. 8, 1981, pp. 336-351.
[52] A.W. Shaw, A.J. Vosper, J. Chem. Soc., Faraday Trans. 1, vol. 73, 1977, pp. 1239-1244.
[53] C.J. C., L.B.N. E., Antioxidants & Redox Signaling, vol. 29, 2018, pp. 1809-1829.
[54] M.W. Foster, J.A. Cowan, Journal of the American Chemical Society, vol. 121, American Chemical Society, 1999, pp. 4093-4100.
[55] K.A. Johnson, M.F.J.M. Verhagen, P.S. Brereton, M.W.W. Adams, I.J. Amster, Analytical Chemistry, vol. 72, American Chemical Society, 2000, pp. 1410-1418.
[56] M. Jia, S. Sen, C. Wachnowsky, I. Fidai, J.A. Cowan, V. Wysocki, Angewandte Chemie International Edition, vol. n/a, John Wiley & Sons, Ltd, 2020.
[57] J. Bourassa, B. Lee, S. Bernard, J. Schoonover, F.C. Ford, Inorganic Chemistry, vol. 38, American Chemical Society, 1999, pp. 2947-2952.
[58] H. Nakajima, M. Yasuda, K. Chiba, A. Baba, Chemical Communications, vol. 46, The Royal Society of Chemistry, 2010, pp. 4794-4796.
Chemistry, vol. 50, American Chemical Society, 1985, pp. 5795-5802.
[60] B. Genorio, T. He, A. Meden, S. Polanc, J. Jamnik, J.M. Tour, Langmuir, vol. 24, American Chemical Society, 2008, pp. 11523-11532.
[61] H.R. Hoveyda, R.H. Holm, Inorganic Chemistry, vol. 36, American Chemical Society, 1997, pp. 4571-4578.
[62] W. Henderson, J.S. McIndoe, Mass Spectrometry of Inorganic, Coordination and Organometallic Compounds, John Wiley & Sons, Ltd, 2005, pp. 127-173.
[63] M. Lewin, K. Fisher, I. Dance, Chemical Communications, The Royal Society of Chemistry, 2000, pp. 947-948.
[64] J.L. Hess, C.-H. Hsieh, J.H. Reibenspies, M.Y. Darensbourg, Inorganic Chemistry, vol. 50, American Chemical Society, 2011, pp. 8541-8552.
[65] T. Nagano, K. Yoshikawa, M. Hirobe, Tetrahedron Letters, vol. 21, 1980, pp. 297-300.
[66] B. Zhang, J.C. Crack, S. Subramanian, J. Green, A.J. Thomson, N.E. Le Brun, M.K. Johnson, Proceedings of the National Academy of Sciences, vol. 109, 2012, pp. 15734-15739.
[67] Y. Nicolet, R. Pohac, L. Martin, J.C. Fontecilla-Camps, Proceedings of the National Academy of Sciences, vol. 110, 2013, pp. 7188.
[68] E.L. Dodd, J.C. Crack, A.J. Thomson, N.E. Le Brun, in: T. Rouault (Ed.), Iron-Sulfur Clusters in Chemistry and Biology. Volume 1 Characterization, Properties and Applications, vol. 1, De Gruyter, Berlin, Boston, 2017, pp. 387-438.
[69] J. Fitzpatrick, H. Kalyvas, J. Shearer, E. Kim, Chemical Communications, vol. 49, The Royal Society of Chemistry, 2013, pp. 5550-5552.
[70] J. Fitzpatrick, E. Kim, Inorganic Chemistry, vol. 54, American Chemical Society, 2015, pp. 10559-10567.
[71] J. Fitzpatrick, E. Kim, Accounts of Chemical Research, vol. 48, American Chemical Society, 2015, pp. 2453-2461.
[72] H. Beinert, R.H. Holm, E. Münck, Science, vol. 277, 1997, pp. 653-659.
[73] C. Zhou, J.W. Raebiger, B.M. Segal, R.H. Holm, Inorganica Chimica Acta, vol. 300-302, 2000, pp. 892-902.

Erin L. Dodd: Project development and design, protein preparation, synthesis, characterization, reactivity studies (mass spectrometry, spectroscopy, etc), data analysis, writing.

Nick E. Le Brun: Project development and design, kind provision of space and equipment, advice.

☐The authors declare that they have no known competing financial interests or personal relationships that could have appeared to influence the work reported in this paper.

☒The authors declare the following financial interests/personal relationships which may be considered as potential competing interests:

Erin L. Dodd reports financial support was provided by The Royal Society. Nick E. Le Brun reports financial support was provided by Biotechnology and Biological Sciences Research Council. co-author Nick E. Le Brun is listed as a member of the editorial board of the Journal of Inorganic Biochemistry, which is the journal to which I am submitting. If there are other authors, they declare that they have no known competing financial interests or personal relationships that could have appeared to influence the work reported in this paper.

This manuscript describes an investigation of the role played by the unusual carboxylate ligand in the nitrosylation of the [4Fe-4S] cluster of the NO-sensing bacterial protein NsrR. A two-pronged approach, following the reaction of NO with: 1. variants of NsrR from *Streptomyces coelicolor* varied at the ligand site, and 2. biomimetic synthetic model cluster complexes, showed greater control of the mechanism of nitrosylation, and longer lived intermediates, in the site-differentiated cluster.

Highlights

- Side-by-side study of nitrosylation of protein- and synthetic cluster model [4Fe-4S] species
- Understanding of mechanistic control in NO-sensor NsrR from *Streptomyces coelicolor*
- Effect of cluster coordination sphere on nitrosylation mechanism / mechanistic control
- Observation of a thiolate-bound mononitrosylated synthetic [4Fe-4S] cluster as key intermediate